



**University of
Zurich**^{UZH}

**Zurich Open Repository and
Archive**

University of Zurich
University Library
Strickhofstrasse 39
CH-8057 Zurich
www.zora.uzh.ch

Year: 2011

Noise-Induced Modulation of the Relaxation Kinetics around a Non-Equilibrium Steady State of Non-Linear Chemical Reaction Networks

Ramaswamy, Rajesh ; Sbalzarini, Ivo F ; González-Segredo, Nérido

Abstract: Stochastic effects from correlated noise non-trivially modulate the kinetics of non-linear chemical reaction networks. This is especially important in systems where reactions are confined to small volumes and reactants are delivered in bursts. We characterise how the two noise sources confinement and burst modulate the relaxation kinetics of a non-linear reaction network around a non-equilibrium steady state. We find that the lifetimes of species change with burst input and confinement. Confinement increases the lifetimes of all species that are involved in any non-linear reaction as a reactant. Burst monotonically increases or decreases lifetimes. Competition between burst-induced and confinement-induced modulation may hence lead to a non-monotonic modulation. We quantify lifetime as the integral of the time autocorrelation function (ACF) of concentration fluctuations around a non-equilibrium steady state of the reaction network. Furthermore, we look at the first and second derivatives of the ACF, each of which is affected in opposite ways by burst and confinement. This allows discriminating between these two noise sources. We analytically derive the ACF from the linear Fokker-Planck approximation of the chemical master equation in order to establish a baseline for the burst-induced modulation at low confinement. Effects of higher confinement are then studied using a partial-propensity stochastic simulation algorithm. The results presented here may help understand the mechanisms that deviate stochastic kinetics from its deterministic counterpart. In addition, they may be instrumental when using fluorescence-lifetime imaging microscopy (FLIM) or fluorescence-correlation spectroscopy (FCS) to measure confinement and burst in systems with known reaction rates, or, alternatively, to correct for the effects of confinement and burst when experimentally measuring reaction rates

DOI: <https://doi.org/10.1371/journal.pone.0016045>

Posted at the Zurich Open Repository and Archive, University of Zurich

ZORA URL: <https://doi.org/10.5167/uzh-79203>

Journal Article

Accepted Version

Originally published at:

Ramaswamy, Rajesh; Sbalzarini, Ivo F; González-Segredo, Nérido (2011). Noise-Induced Modulation of the Relaxation Kinetics around a Non-Equilibrium Steady State of Non-Linear Chemical Reaction Networks. PLoS ONE, 6(1):e16045.

DOI: <https://doi.org/10.1371/journal.pone.0016045>

Noise-Induced Modulation of the Relaxation Kinetics around a Non-Equilibrium Steady State of Non-Linear Chemical Reaction Networks

Rajesh Ramaswamy¹, Ivo F. Sbalzarini², Nérido González-Segredo^{3,4}

Institute of Theoretical Computer Science, ETH Zürich, CH-8092 Zürich, Switzerland and

Swiss Institute of Bioinformatics, ETH Zürich, CH-8092 Zürich, Switzerland

Abstract

Stochastic effects from correlated noise non-trivially modulate the kinetics of non-linear chemical reaction networks. This is especially important in systems where reactions are confined to small volumes and reactants are delivered in bursts. We characterise how the two noise sources confinement and burst modulate the relaxation kinetics of a non-linear reaction network around a non-equilibrium steady state. We find that the lifetimes of species change with burst input and confinement. Confinement increases the lifetimes of all species that are involved in any non-linear reaction as a reactant. Burst monotonically increases or decreases lifetimes. Competition between burst-induced and confinement-induced modulation may hence lead to a non-monotonic modulation. We quantify lifetime as the integral of the time autocorrelation function (ACF) of concentration fluctuations around a non-equilibrium steady state of the reaction network. Furthermore, we look at the first and second derivatives of the ACF, each of which is affected in opposite ways by burst and confinement. This allows discriminating between these two noise sources. We analytically derive the ACF from the linear Fokker–Planck approximation of the chemical master equation in order to establish a baseline for the burst-induced modulation at low confinement. Effects of higher confinement are then studied using a partial-propensity stochastic simulation algorithm. The results presented here may help understand the mechanisms that deviate stochastic kinetics from its deterministic counterpart. In addition, they may be instrumental when using fluorescence-lifetime imaging microscopy (FLIM) or fluorescence-correlation spectroscopy (FCS) to measure confinement and burst in systems with known reaction rates, or, alternatively, to correct for the effects of confinement and burst when experimentally measuring reaction rates.

Introduction

The workhorse of much research on chemical kinetics has been macroscopic reaction-rate equations. These are deterministic, mean-field descriptions that treat molecular populations as continuous and use macroscopically determined rate constants. Hence they do not always provide an accurate description of reaction kinetics [1,2]. This lack of accuracy occurs for nonlinear reactions if the population (copy number) of the various chemical species is small enough such that standard errors are not negligible [3–9]. These conditions are found, for example, in confined systems that fall short of the thermodynamic limit [10], and in driven reaction systems [11–13]. In them, the noise due to molecular discreteness becomes apparent and acquires correlations to give a departure from the behaviour predicted by macroscopic reaction-rate equations [1,12,14–16].

In this paper we study a representative model of non-linear reaction networks, kept at a non-equilibrium steady state by exchanging input and output with an external reservoir. The input is done in bursts. In a reaction system with burst input $\emptyset \xrightarrow{k} bA$ into a reactor of finite volume Ω (k is the macroscopic reaction rate), the variance at a non-equilibrium steady state is $O(b/\Omega)$ (see Eq. (18) in “Effect

¹Email: rajeshr@ethz.ch

²Email: ivos@ethz.ch

³Email: nelidog@ethz.ch

⁴Now at: Centre for Nonlinear Phenomena and Complex Systems, Faculté des Sciences, CP 231, Université Libre de Bruxelles, B-1050 Brussels, Belgium

of volume and burst on the concentration variance” in “Materials and Methods”). Several environments might host mechanisms of the type burst-input–non-burst-output by non-diffusive, driven processes, such as vesicular traffic in the biological cell [17]. The input–output may be to and from compartments that have physical walls or interstices caused by excluded volume [18]. In particular, this mechanism occurs in the dynamics of membrane-protein domains (rafts) in contact with a metabolic network [19, 20]. Reaction-rate equations do not discriminate (i) between a stoichiometric (burst) input $\emptyset \xrightarrow{k} bA$ and a non-stoichiometric input $\emptyset \xrightarrow{bk} A$, or (ii) the volume Ω of the compartment.

We account for these effects via chemical master equations, which can be solved using analytical approximations [6, 21, 22] or generating exact trajectories using Gillespie-type stochastic simulation algorithms (SSAs) [23, 24]. We use these tools to study the effects of two noise sources — (i) low copy number as created by finite volume Ω and (ii) input stoichiometry b — on the relaxation kinetics of non-linear reaction networks. Specifically, we study the time autocorrelation function (ACF) of concentration fluctuations around a non-equilibrium steady state via its integral (lifetime) and derivatives. For this we use (i) a linear-noise, Fokker–Planck approximation to the master equation via a van Kampen expansion in the system volume [21, 22] and (ii) the full master equation via the partial-propensity direct method (PDM) [24, 25].

We show that the lifetime of chemical species is modulated by burst input b and volume Ω (or confinement Ω^{-1}). We quantify lifetime by the autocorrelation time of the concentration fluctuations. This autocorrelation is measured in fluorescence-lifetime imaging microscopy (FLIM) or fluorescence-correlation spectroscopy (FCS) [26]. Analysis of FLIM and FCS spectra, however, is based on deterministic reaction rate equations, which are only valid in large volumes and do not reflect the effect of burst input. We show that confinement increases the lifetime of all reactants in a non-linear reaction. Burst either increases or decreases the lifetime. Furthermore, we show that the derivatives of the ACF of the concentration fluctuations are affected in opposite ways by burst b and confinement Ω^{-1} , thus discriminating between the two noise source. This directly links the present results to experimental application in two ways: (i) Knowing the lifetime modulation introduced by confinement and burst allows accurately measuring reaction rates in experimental systems. Lifetime is a measure of reaction flux, which is a function of the reaction rates. (ii) Derivatives of the ACF can be used to discriminate between the confinement- and burst-induced effects.

We hence believe that our findings are useful in order to (i) Use FLIM or FCS to measure input stoichiometry b and volume Ω when reaction rates are known. (ii) Correct for the effects of burst input and volume when experimentally measuring reaction rates. (iii) Understand the mechanisms that deviate stochastic kinetics from its deterministic counterpart and choose the right level of description when modelling non-linear reaction networks. (iv) Account for the influences of confinement and burst in formulating coarse-grained governing equations of non-linear reaction models.

We are not aware of previous works tackling the relaxation kinetics of stochastic non-linear reaction networks around a non-equilibrium steady state at arbitrarily low copy number as created by finite volume and driven by a burst input mechanism.

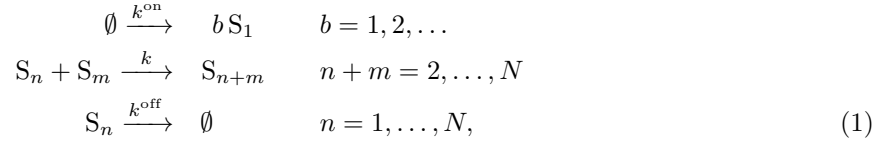
In Section “Model” we introduce the model and its assumptions. Section “Low confinement: the linear-noise approximation” expands the master equation in a van Kampen volume expansion in the linear-noise approximation. From this we study time autocorrelations, which show modulation by the burst b alone. In Section “Beyond the linear-noise approximation: the full master equation”, using the PDM SSA we numerically generate population trajectories of the full master equation as system volume Ω is shrunk and burst b is increased. The autocorrelations of these trajectories have those of the linear-noise approximation as a baseline. Section “Discussion” provides analysis and Section “Conclusions” concludes.

Model

As a representative model of non-linear reaction networks out of equilibrium we consider driven colloidal aggregation, for three reasons: First, it is a complete model since this reaction network comprises all three types of elementary reactions: bimolecular, source (input), and unimolecular [27], rendering the results obtained here valid also for other reaction networks. Second, it is a well-characterised model as it has been studied for decades, notably from the 1916 works of Smoluchowski on coagulation and fragmentation. Third, it is a relevant model for many real-world phenomena of practical importance, e.g., in the biological cell (receptor oligomerisation, protein and prion-peptide aggregation, cytoskeletal actin & tubulin polymerisation), in nanotechnology (nano-particle clustering, colloidal crystallisation), in food engineering and the oil industry (emulsion stabilisation, emulsification in porous media), and in metallurgy (dealloying).

We use the chemical master equation to solve the reaction kinetics, neglecting molecular aspects underlying nucleation and growth. Our system is spatially homogeneous (well-stirred) as we disregard structural, spatial, or solvent effects. We also factor out the role of (i) densification upon decrease in system volume, as the total volume fraction is kept constant, and (ii) conformational kinetics, as we do not consider intra-molecular degrees of freedom. In addition, we study our system at a steady state that may be arbitrarily far away from thermodynamic equilibrium as our results do not impose any (semi-)detailed balance condition on the SSA's Markov chain.

Denoting aggregates containing n particles as species S_n the aggregation reaction network is:



where the k 's are macroscopically measurable reaction rates as opposed to specific probability rates [23,24]. This system describes the aggregation of monomers S_1 into multimers S_n of maximum size N . Monomers are input into the finite reaction volume in bursts of arbitrary size b . They then form dimers, which can further aggregate with other monomers or multimers to form larger aggregates. Aggregation of multimers happens at a constant rate k for all possible combinations of multimer sizes n and m . In addition, aggregates of any size are taken out of the reaction volume at constant rate k^{off} , enabling the system to reach a non-equilibrium steady state. For simplicity we consider constant k 's. The model could readily be generalized to reaction rates k_{nm} that depend on the aggregate sizes [21, 28]. We chose not to include this generalisation in order to keep the presentation and notation simple, and to establish the baseline effects of volume and burst in the absence of size dependence. Our results will remain valid also in models that explicitly account for size-dependent reaction rates.

If X_n is an extensive variable denoting the number of aggregates of size n (population of S_n) contained in the system volume Ω , the concentration is $x_n \equiv X_n/\Omega$. The master equation and its macroscopic counterpart for our model system are then given by Eqs. (20) and (21), respectively (see ‘‘Chemical master equation and its macroscopic counterpart for burst-input aggregation’’ in ‘‘Materials and Methods’’). We impose that the average total volume fraction $\phi \equiv \sum_{n=1}^N n v \langle x_n \rangle_s$ should not vary in time, where v is the volume of each particle and $\langle \cdot \rangle_s$ denotes average at steady state. This is satisfied if particle (monomer) influx $b c^{\text{on}}$ and particle efflux $\Omega \sum_n n \langle x_n \rangle_s c^{\text{off}}$ balance each other, where the c 's are specific probability rates, $c^{\text{on}} = \Omega k^{\text{on}}$ and $c^{\text{off}} = k^{\text{off}}$. This leads to the mass-balance condition

$$v b k^{\text{on}} / k^{\text{off}} = \phi. \tag{2}$$

We isolate the role of Ω from that of densification by keeping ϕ constant as we vary Ω across systems of fixed b , v , and k^{off} . We isolate the role of stoichiometry b from that of influx $b k^{\text{on}} \Omega$ by keeping $b k^{\text{on}}$

constant as we vary b and Ω across systems of fixed v and k^{off} . Under mass balance and $b k^{\text{on}} = \text{const.}$, the macroscopic Eq. (21) (see “Chemical master equation and its macroscopic counterpart for burst-input aggregation” in “Materials and Methods”) is insensitive to burst b and confinement Ω^{-1} for a fixed k . Hence the deviation in our stochastic kinetics from the macroscopic kinetics arises solely due to noise sources b and Ω^{-1} .

The master equation associated with the reactions in Eq. (1) provides the time evolution of the probability distribution $P(\mathbf{X}, t)$ of the population vector $\mathbf{X} \equiv (X_1, \dots, X_N)$ (see Eq. (20) in “Chemical master equation and its macroscopic counterpart for burst-input aggregation” in “Materials and Methods”). We solve it approximately using (i) a van Kampen expansion at the linear-noise, Fokker–Planck level, and (ii) numerically generating exact trajectories of the master equation using an SSA. We compute the ACF of the concentration of species S_n at steady state as

$$C_{nn}(t) \equiv \langle \widetilde{x}_n(0) \widetilde{x}_n(t) \rangle_s / \sigma_{x_n}^2. \quad (3)$$

Here, 0 is a time origin at steady state, i.e. after the initial relaxation period $-\infty < t < 0$, where $-\infty$ represents an arbitrary origin in the past. $\langle \cdot \rangle_s$ is an average at steady state over time origins and independent stochastic trajectories, $\widetilde{x}_n \equiv x_n - \langle x_n \rangle_s$ is the fluctuation, and $\sigma_{x_n}^2 = \langle \widetilde{x}_n(0) \widetilde{x}_n(0) \rangle_s$ is the variance.

We compute the correlation time of an aggregate of size n as

$$\tau_n \equiv \int_0^\infty C_{nn}(t) dt \approx \int_0^{t_n^\times} C_{nn}(t) dt, \quad (4)$$

where t_n^\times is the first zero crossing. This is a measure of the average decay time and we shall refer to it as lifetime of species S_n . We shall show (in “Low confinement: the linear-noise approximation” in “Results”) that the ACF may become negative due to oscillations, which may make Eq. (4) unsuitable as a measure of a correlation time. The frequency of these oscillations, however, is small enough for our SSA trajectories to justify the approximation in Eq. (4).

We also compute the decay-rate function of the ACF as

$$\chi_n(t) \equiv -\frac{d}{dt} C_{nn}(t) \quad (5)$$

and the initial curvature of the ACF

$$Z_n \equiv \frac{d^2}{dt^2} C_{nn}(0). \quad (6)$$

These quantities serve as (curve) characteristics to study the effects of b and Ω on the kinetics. In addition, they provide a connection with experiments since they can directly be calculated from standard FCS or FLIM read-outs.

In the following, we limit ourselves to a trimer system ($N = 3$) as the simplest aggregation reaction network that comprises all elementary reactions: source reactions, unimolecular reactions, and the two types of bimolecular reactions: homodimerisation and heterodimerisation. This makes the characteristics of the ACF as a function of burst and confinement applicable also for $N > 3$ and for other non-linear reaction networks around a non-equilibrium steady state. In our model, we set $k^{\text{off}} = 1$, $v = 0.01$, $k = 1$, and $\phi = 0.1$. We also limit ourselves to (b, Ω) -regimes where population fluctuations are not larger than their mean. We estimate the bounds of this regime as follows: The mean number of particles at steady state is $\phi\Omega/v = 10\Omega$. From Eq. (18) we see that the standard deviation at steady state without any aggregation, i.e. for a system containing only monomers, is proportional to $(b\phi\Omega/(2v))^{1/2}$ (see “Effect of volume and burst on the concentration variance” in “Materials and Methods”). We impose the mean as an upper bound for twice the standard deviation. This imposes a b -dependent lower bound on the system volume: $\phi\Omega/v > 2b$.

Results

Low confinement: the linear-noise approximation

In this section we analytically approximate the master equation associated with the reactions in Eq. (1) by a linear-noise (LN) Fokker–Planck equation [22]. The LN approximation of the master equation is valid at low confinement, i.e., for finite but large enough system volumes. We do this in order to (i) obtain a baseline kinetics on top of which to lay out the full-master-equation kinetics provided in the next section (see “Beyond the linear-noise approximation: the full master equation”), (ii) obtain analytical functions for the ACF, and (iii) reach the large-volume, low-confinement limit where modulation of the ACF by Ω vanishes, thus isolating the dependence on b .

For the sake of conciseness we provide details of the procedure in “Materials and Methods” (see “Linear-noise approximation of the chemical master equation for burst-input aggregation”). The approximation consists of retaining leading-order terms in a Taylor expansion of $P(\mathbf{X}, t)$ in the small parameter $\Omega^{-1/2}$. The latter enters after assuming that the noise scales with system volume Ω as $\widetilde{x}_n = \Omega^{-1/2}\epsilon_n$, where ϵ_n is a random variable evolved by a master equation [15, 21, 22].

In the LN approximation, (i) the noise ϵ_n is Gaussian, (ii) the mean $\langle x_n \rangle$ obeys a macroscopic reaction-rate equation, and (iii) the moments of $P(\mathbf{X}, t)$, including the ACF, do not depend on Ω [22]. Despite this, the LN approximation remains useful as there the moments do depend on the burst b , as we show in this section.

For the sake of simplicity we restrict ourselves to $N = 3$. Considering that in the LN approximation the covariances $\langle \widetilde{x}_n \widetilde{x}_m \rangle_s$ coincide with the second moments $\langle x_n x_m \rangle_s$ because the mean noise is zero, we solve the time evolution of the first and second moments (See Eqs. (28), (29) in “Linear-noise approximation of the chemical master equation for burst-input aggregation” in “Materials and Methods”) around steady state to obtain the ACF at steady state,

$$\begin{aligned} C_{11}(t) &= f_{1,1}e^{-\Gamma_1 t} + f_{1,2}e^{-\Gamma_2 t} \\ C_{22}(t) &= f_{2,1}e^{-\Gamma_1 t} + f_{2,2}e^{-\Gamma_2 t} \\ C_{33}(t) &= f_{3,1}e^{-\Gamma_1 t} + f_{3,2}e^{-\Gamma_2 t} + f_{3,3}e^{-\Gamma_3 t}. \end{aligned} \quad (7)$$

The coefficient $f_{i,j}$, $i, j = 1, \dots, N$, is a ratio of two functions that are linear in the covariances. The rates Γ_j , $j = 1, \dots, N$, are

$$\begin{aligned} 2\Gamma_1 &\equiv 2k^{\text{off}} + 3k\bar{x}_1^s + k\bar{x}_2^s - k\sqrt{-3\bar{x}_1^{s2} + 6\bar{x}_1^s\bar{x}_2^s + \bar{x}_2^{s2}} \\ 2\Gamma_2 &\equiv 2k^{\text{off}} + 3k\bar{x}_1^s + k\bar{x}_2^s + k\sqrt{-3\bar{x}_1^{s2} + 6\bar{x}_1^s\bar{x}_2^s + \bar{x}_2^{s2}} \\ \Gamma_3 &\equiv k^{\text{off}}, \end{aligned} \quad (8)$$

where \bar{x}_n^s is the steady-state macroscopic concentration of species S_n obtained by solving Eq. (21). Note that Γ_1 and Γ_2 may have an imaginary part, which will give the ACF an oscillatory contribution introducing anticorrelation at late times. By integrating Eq. (7) over $[0, \infty)$ we get the lifetimes,

$$\begin{aligned} \tau_1 &= f_{1,1}\Gamma_1^{-1} + f_{1,2}\Gamma_2^{-1} \\ \tau_2 &= f_{2,1}\Gamma_1^{-1} + f_{2,2}\Gamma_2^{-1} \\ \tau_3 &= f_{3,1}\Gamma_1^{-1} + f_{3,2}\Gamma_2^{-1} + f_{3,3}\Gamma_3^{-1}, \end{aligned} \quad (9)$$

where the integrals of Eq. (7) from their first zero-crossings up to infinity are negligibly small ($\text{Re } \Gamma_n \gtrsim 4 \text{Im } \Gamma_n$). The corresponding integrals over $[t_n^\times, \infty)$ for the SSA-computed ACFs remain small, as mentioned in the Section “Model”.

The pre-factor $f_{i,j}$, $i, j = 1, \dots, N$, is a ratio of two functions linear in the burst b because each covariance is linear in b . This is seen by solving Eq. (29) (see “Linear-noise approximation of the chemical

master equation for burst-input aggregation” in “Materials and Methods”) at steady state under mass balance Eq. (2). As a consequence, $f_{i,j}$, $i, j = 1, \dots, N$, becomes b -independent at large enough b , and so do the lifetimes. Figure 1(a) shows how the lifetimes depend on burst. As burst increases from the no-burst case $b = 1$, monomer lifetimes decrease and multimer lifetimes increase. As seen from Eq. (9), the lifetimes become b -independent at large enough b , Fig. 1(b). This thus defines a high- b region above $b \approx 300$. It can also be seen from the general form of Eq. (9) for N species that, for a non-linear reaction network at a non-equilibrium steady state, τ_n will either increase or decrease with b , except in zero-measure regions of parameter space where τ_n stays constant.

Figure 2 shows the decay-rate function $\chi_n(t)$ for several burst values. For monomers, $\chi_1(t)$ remains monotonic as burst increases, with its maximum at $t = 0$. For dimers, $\chi_2(t)$ becomes non-monotonic above a threshold burst $b \approx 10$, while for trimers the threshold sets in before, at $b \approx 6$. In other words, the decay-rate function of the non-aggregating multimers (trimers) is more sensitive to burst than that of the aggregating multimers (dimers). Note that the maximum that develops shifts from being at $t = 0$ towards later times as burst increases the time $t_n^{X, \max}$ at which $\chi_n(t)$ reaches its maximum. We define $t_n^{X, \max}$ as the time of fastest decay since the (absolute value of the) ACF slope is maximum at this time.

In this section we have calculated the ACF from the linear-noise approximation of the master equation, from which we obtained the lifetimes. We observed that the ACF is a superposition of exponentials with pre-factors modulated by the driving, thereby obtaining the baseline of the burst-induced modulation of the kinetics.

Beyond the linear-noise approximation: the full master equation

We showed in the previous section how the ACF depends on burst in the low-confinement limit. In this section we show how higher confinement further modulates this ACF. We compute the stochastic trajectories of the populations X_n as given by the full master equation to show that shrinking the volume at high-enough confinement further modulates lifetimes and the time of fastest decay. In addition, we introduce the ACF’s initial curvature as a further characteristic.

To generate stochastic trajectories from the full master equation we use an efficient SSA [24]. For each parameter set we generate an ensemble of 20 000 independent trajectories at steady state. Each trajectory is roughly $20(k^{\text{off}})^{-1}$ long, about 4 000 time steps of step length $0.005(k^{\text{off}})^{-1}$. The initial condition for each trajectory is $X_n(-\infty) = 0$, where $-\infty$ represents an arbitrary origin in the past and $-\infty < t < 0$ is a period of relaxation to steady state.

Lifetime

Figure 3 shows the lifetimes $\tau_n(\Omega)$ as a function of volume Ω for both no burst $b = 1$ and a burst value in the high-burst region observed in the LN limit, $b = 500$. We see that shrinking Ω increases τ_1 and τ_2 , but not τ_3 , and that this effect is more appreciable at larger Ω as burst b increases.

Figure 4 shows maps of lifetime versus volume for a burst range. The trimers’ map shows that volume does not affect lifetime, as also seen in Fig. 3. Figure 4 shows that for monomers and dimers, increasing burst b extends the Ω -interval over which the lifetime varies with Ω . This can also be seen in Fig. 3. In other words, burst seems to act as an amplifier (multiplicative-noise parameter) for confinement-induced lifetime modulation.

The monomer lifetime τ_1 deserves special attention because it is the only lifetime that is non-monotonic in the burst b , see Fig. 4(a). For any Ω fixed in the interval $100 \lesssim \Omega \lesssim 1000$, τ_1 decreases with b and then increases back for b beyond some threshold b_1^- . The threshold b_1^- , in turn, decreases with confinement Ω^{-1} . The non-monotonicity of $\tau_1(b)$ is a high-confinement effect because it does not occur in the linear-noise Fokker–Planck limit, see Fig. 1. The existence of the threshold b_1^- , nonetheless, is not surprising because for monomers, confinement and burst cause opposing modulations: confinement *increases* lifetime

whereas, as seen from the LN limit, burst *decreases* it. Since burst amplifies the confinement-induced modulation of the lifetime, it acts as a $-/+$ switch for it.

We can also view the problem from the perspective of how confinement affects burst-induced lifetime modulation: varying b while we fix Ω below the LN limit, see Fig. (4). In other words, by looking into a hypothetical volume-dependent, high-confinement version of Eq. (9). Note also that the lifetimes $\tau_2(b)$ and $\tau_3(b)$ are the only lifetimes increasing with burst b in the LN limit. Recall that further confinement Ω^{-1} allows the decreasing function $\tau_1(b)$ to acquire a slope of the same sign of that of $\tau_2(b)$ and $\tau_3(b)$ for large enough burst b . This suggests that confinement Ω^{-1} is an amplifier of burst-induced lifetime modulation. This amplification, in turn, must result from $O(\Omega^{-\alpha})$ terms entering $f_{i,j}$, $i, j = 1, \dots, N$, and/or $O(\Omega^\alpha)$ terms entering Γ_j , $j = 1, \dots, N$, in Eq. (9) for some $\alpha > 0$.

In summary, we have shown that confinement Ω^{-1} increases the lifetime of all species that are reactants in a bimolecular reaction, i.e., trimers are insensitive to confinement. Confinement-induced modulation lays on top of the burst-induced modulation seen in the LN limit. It provides an effective modulation that may lead to non-monotonic behaviour.

Derivatives of the ACF

Figure 5 shows representative samples of how the decay-rate function $\chi_n(t)$ responds to volume shrinking at burst $b = 500$. This burst value corresponds to a monotonicity post-threshold value for the multimers ($n = 2, 3$) at low confinement, see Fig. 2. Our aim here is to study how confinement alters this low-confinement behaviour. We look for qualitative features that correlate with changes in volume Ω and stoichiometry b . These features may possibly be used to develop quantitative methods to characterise local volume and stoichiometry from FCS-sampled ACFs.

From Fig. 5 we can see that for monomers, $\chi_1(t)$ is monotonic. For multimers ($n = 2, 3$), $\chi_n(t)$ is non-monotonic, making $t_n^{\chi, \max} > 0$. This change in monotonicity is a purely burst-induced modulation, as opposed to confinement-induced, and exists already in the LN limit (see ‘‘Low confinement: the linear-noise approximation’’). Note that confinement reduces $t_n^{\chi, \max}$, as opposed to burst, which increases it, see Fig. 2.

Up to now we have studied two-dimensional datasets $\{(t, \chi_n)\}$. To facilitate feature detection in an FCS experiment, it would be desirable to reduce dimensionality from two dimensions to one. To this end we now study the ACF initial curvature Z_n . Since $Z_n = -\frac{d}{dt}\chi_n(0)$, from Fig. 5 we see that Z_n is monotonic for all species as the volume shrinks.

Figure 6 shows the ACF initial curvature Z_n for burst and volume ranges. For monomers, confinement *increases* Z_1 , more noticeably at larger burst. Moreover, $Z_1 > 0$, reflecting the monotonicity of $\chi_1(t)$. For multimers ($n = 2, 3$), on the contrary, confinement *reduces* the ACF initial curvature from a positive to a negative value as we go from the small- b -large- Ω region to the large- b -small- Ω region. This reflects the non-monotonicity of $\chi_n(t)$, $n > 1$, beyond a burst threshold. In other words, the change of monotonicity is a purely burst-induced modulation also at high confinement. There is no qualitative difference between aggregating ($n = 2$) and non-aggregating ($n = 3$) multimers.

Discussion

In Table 1 we summarise the behaviour of the most relevant characteristics we studied, which can be obtained *a posteriori* from standard FCS or FLIM read-outs. This table may serve as a reference for contrasting burst-induced and confinement-induced modulations and be useful for later studies of the mechanisms behind them. An immediate use may be to help discern whether the noise source is burst-induced or confinement-induced.

The presence of oscillations implies that care must be taken when calculating lifetimes. We have calculated them by integrating the ACF up to its first zero crossing. This is only justified if the frequency

of the oscillations is low enough, as is our case, see Eq. (4). For reaction networks showing non-negligible frequencies, calculating lifetimes as the mean of the lifetime distribution could be considered. This distribution could be obtained from the distribution of the so-called “time to the next reaction”, as generated by the SSA [23,24], however requiring a suitable definition for lifetime as a function of it.

Finally, including scission as a backward reaction in Eq. (1) would not modify the qualitative behaviour presented in this paper. This is because scission is a unimolecular reaction, whose reaction degeneracy, and hence its propensity, is linear in the population while the degeneracy for aggregation is non-linear [23,24]. Consequently, scission would modify the populations at the same rate for all reactants S_{n+m} and would not introduce any additional non-linearities. This is also confirmed by SSA simulations (data not shown). Note that scission is not negligible for aggregates of low enough interfacial tension, whose equilibrium in the absence of driving is not totally displaced to the right.

Conclusions

We have characterised fundamental properties of the relaxation kinetics of a non-linear stochastic reaction network around a non-equilibrium steady state. We have chosen as a model a confined, open colloidal aggregation system of finite volume Ω . The system is driven by a monomer influx in bursts of b monomers and a non-burst multimer outflux. Specifically, we studied the trimer aggregation network as the simplest aggregation network comprising all types of elementary reactions. This makes our observations on the relaxation kinetics applicable also to larger aggregation networks and to other non-linear reaction networks around a non-equilibrium steady state. We studied the role of (i) low copy number created by confinement Ω^{-1} at constant volume fraction, and (ii) burst influx b . Both of these are noise sources that increase concentration fluctuations.

We accounted for these stochastic effects using (i) a linear-noise, Fokker–Planck approximation, valid in the low-confinement limit, and (ii) exact trajectories of the master equation from a stochastic simulation algorithm, modelling high confinement. We used the time autocorrelation function (ACF) of species concentrations to study the relaxation kinetics towards the non-equilibrium steady state.

We have proposed the following curve characteristics to study the response of the ACF of a species n to confinement (inverse volume) and burst: (i) the lifetime $\tau_n = \int_0^\infty C_{nn}(t)dt$, (ii) the decay-rate function $\chi_n(t) = -\frac{d}{dt}C_{nn}(t)$, and (iii) the ACF’s initial curvature $Z_n = \frac{d^2}{dt^2}C_{nn}(0)$.

We observed that increasing burst b monotonically increases or decreases the lifetimes of all species, except in zero-measure regions of parameter space where they stay constant. On the other hand, confinement Ω^{-1} increases the lifetime of those species undergoing bimolecular reactions (monomers and dimers), but does not modulate those undergoing only unimolecular reactions (trimers). This can lead to a competition between confinement-induced and burst-induced modulations. From these observations we hypothesise that the ACF is modulated through terms of the form $b^\alpha \Omega^{-\beta}$ for some $\alpha \geq 0$, $\beta \geq 0$.

Burst alone is responsible for making $\chi_n(t)$ non-monotonic for some species. The peak in the non-monotonic $\chi_n(t)$, reflected by Z_n , is shifted in opposite directions by burst b and confinement Ω^{-1} .

We believe that our results are useful to measure volume and burst in systems with known reaction rates, or, alternatively, correct for the effects of volume and burst when experimentally measuring reaction rates using fluorescence-lifetime imaging microscopy (FLIM) or fluorescence-correlation spectroscopy (FCS). Furthermore, our results help understand the mechanisms that deviate the stochastic kinetics of non-linear reaction networks at high confinement and burst from their deterministic counterpart.

Materials and Methods

Effect of volume and burst on the concentration variance

Consider the following chemical reaction



Also consider the step operator \mathbb{E}^r acting on a function g of the population X of S_1 such that $\mathbb{E}^r g(X) = g(X + r)$. The master equation for the stochastic evolution of reaction (Eq.10) can then be written as

$$\frac{\partial P(X, t)}{\partial t} = \Omega k^{\text{on}} (\mathbb{E}^{-b} - 1) P + k^{\text{off}} (\mathbb{E} - 1) (X P) \quad (11)$$

where Ω is the volume in which the reaction takes place and $P(X, t)$ is the probability distribution for having X molecules of S_1 at time t .

Multiplying Eq. (11) by X and summing over all possible values of X we get the evolution of the mean

$$\frac{d\langle X \rangle}{dt} = \Omega k^{\text{on}} b - k^{\text{off}} \langle X \rangle. \quad (12)$$

We obtain the steady-state mean by setting the time derivative to zero

$$\langle X \rangle_s = \frac{\Omega k^{\text{on}} b}{k^{\text{off}}}. \quad (13)$$

By multiplying Eq. (11) by X^2 and summing up over all possible values of X we get

$$\frac{d\langle X^2 \rangle}{dt} = \Omega k^{\text{on}} b (b + 2\langle X \rangle) - k^{\text{off}} (2\langle X^2 \rangle - \langle X \rangle). \quad (14)$$

By setting the time derivative to zero we see that at steady state

$$\langle X^2 \rangle_s - \langle X \rangle_s^2 = \frac{k^{\text{on}}}{2k^{\text{off}}} b(b + 1)\Omega, \quad (15)$$

which is the population variance. Hence the variance of the concentration, $x = X/\Omega$, at steady state is

$$\sigma_s^2 = \frac{k^{\text{on}}}{k^{\text{off}}} \frac{b(b + 1)}{2\Omega}. \quad (16)$$

Note that $\sigma_s^2 \sim b^2/\Omega$.

Imposing that the average volume fraction $\phi = v \langle x \rangle_s$ is constant at steady state, where v is the volume of a monomer, leads to the mass-balance condition

$$v b k^{\text{on}} / k^{\text{off}} = \phi, \quad (17)$$

see Eq. (2). Fixing k^{off} , v , and ϕ hence fixes the product $b k^{\text{on}}$, which appears in the macroscopic rate equation. The condition (Eq.17) leads to the concentration variance

$$\sigma_s^2 = \frac{\phi}{v} \frac{(b + 1)}{2\Omega} \quad (18)$$

and the mean concentration

$$\langle x \rangle_s = \phi/v. \quad (19)$$

Imposing mass balance thus modifies the scaling of the steady-state variance to b/Ω .

Having a non-linear reaction in Eq. (10) would leave this scaling unchanged as long as the mass-balance condition holds.

Chemical master equation and its macroscopic counterpart for burst-input aggregation

The master equation associated to reactions (Eq. 1) is:

$$\begin{aligned}
\frac{\partial P}{\partial t} &= \Omega k^{\text{on}} (\mathbb{E}_1^{-b} - 1) P \\
&+ \Omega^{-1} k \sum_{n=1}^{\lfloor N/2 \rfloor} \left((\mathbb{E}_n^2 \mathbb{E}_{2n}^{-1} - 1) \left(\frac{1}{2} X_n (X_n - 1) P \right) \right. \\
&\quad \left. + \sum_{m=n+1}^{N-n} (\mathbb{E}_n^1 \mathbb{E}_m^1 \mathbb{E}_{n+m}^{-1} - 1) (X_n X_m P) \right) \\
&+ k^{\text{off}} \sum_{n=1}^N (\mathbb{E}_n^1 - 1) (X_n P),
\end{aligned} \tag{20}$$

where $P = P(\mathbf{X}, t)$ is the joint probability distribution of the population vector $\mathbf{X} \equiv (X_1, \dots, X_N)$ at time t . Ω is the volume of the reaction compartment and \mathbb{E}_n^r is the step operator acting only on functions of X_n such that $\mathbb{E}_n^r g(X_n) = g(X_n + r)$, where $g(X_n)$ is some function of X_n . Note that imposing that the average volume fraction $\phi = \sum_{n=1}^N n v \langle x_n \rangle_s$ is constant at steady state, where v is the volume of a monomer, again leads to the mass-balance condition in Eq. (17).

The macroscopic (i.e., deterministic) counterpart of Eq. (20), valid in the limit of very large volumes [10], is given by

$$\begin{aligned}
\frac{d\bar{x}_n}{dt} &= k^{\text{on}} b \delta_{n,1} \\
&+ \frac{k}{2} \sum_{p=1}^{\lfloor N/2 \rfloor} \sum_{q=p}^{N-p} \bar{x}_p \bar{x}_q (2 - \delta_{p,q}) (\delta_{p+q,n} - \delta_{p,n} - \delta_{q,n}) \\
&- k^{\text{off}} \bar{x}_n,
\end{aligned} \tag{21}$$

where \bar{x}_n is the macroscopic concentration of the aggregate of size n .

Linear-noise approximation of the chemical master equation for burst-input aggregation

Analytically solving Eq. (20) for $P = P(\mathbf{X}, t)$ is intractable since the right-hand side of the equation is non-linear in the populations. This is almost always true for systems involving bimolecular reactions, save very few exceptions. We can, however, follow van Kampen to volume-expand the master equation in the small parameter $1/\sqrt{\Omega}$ [15, 21, 22].

We consider the stochastic quantity $x_n \equiv X_n/\Omega$ to fluctuate around the mean *macroscopic* concentration \bar{x}_n . This is satisfied by the following ansatz

$$X_n \equiv \Omega \bar{x}_n + \sqrt{\Omega} \epsilon_n, \tag{22}$$

where ϵ_n is random, and of non-zero mean in general. From Eq. (22) we see that any function of X_n satisfies $g(X_n + r) = g(\epsilon_n + r/\sqrt{\Omega})$, which allows introducing the volume expansion

$$\mathbb{E}_n^r = \sum_{i=0}^{\infty} \frac{1}{i!} \left(\frac{r}{\sqrt{\Omega}} \right)^i \frac{\partial^i}{\partial \epsilon_n^i}. \tag{23}$$

From Eqs. (22) and (23), Eq. (20) becomes

$$\begin{aligned} \frac{\partial \Pi}{\partial t} - \Omega^{1/2} \sum_{n=1}^N \frac{d\bar{x}_n}{dt} \frac{\partial \Pi}{\partial \epsilon_n} &= \Omega^{1/2} a_1 \Pi + \Omega^0 a_2 \Pi \\ &+ O(\Omega^{-1/2}), \end{aligned} \quad (24)$$

where $\Pi(\epsilon, t) = P(\mathbf{X}, t)$, $\epsilon \equiv (\epsilon_1, \dots, \epsilon_N)$, and a_1, a_2 are differential operators.

To make Eq. (24) a proper expansion in $1/\sqrt{\Omega}$ we impose that terms proportional to $\Omega^{1/2}$ on both sides are equal. Subsequently, equating terms proportional to $\frac{\partial \Pi}{\partial \epsilon_n}$ gives Eq. (21). Then, at $O(\Omega^0)$, we are left with

$$\frac{\partial \Pi}{\partial t} = a_2 \Pi, \quad (25)$$

where a_2 is the operator

$$a_2 \equiv \sum_{n=1}^N \sum_{m=1}^N \left(-A_{n,m} \frac{\partial}{\partial \epsilon_n} \epsilon_m + \frac{1}{2} B_{n,m} \frac{\partial^2}{\partial \epsilon_n \partial \epsilon_m} \right), \quad (26)$$

with $A_{n,m} \equiv B_{n,m} \equiv 0$ if $n + m > N$, otherwise

$$\begin{aligned} A_{n,m} &\equiv k \sum_{p=1}^N \bar{x}_p (\delta_{p+m,n} - \delta_{n,p} - \delta_{m,n}) - \delta_{n,m} k^{\text{off}} \\ B_{n,m} &\equiv \frac{k}{2} \sum_{p=1}^N \sum_{q=1}^N \bar{x}_p \bar{x}_q (\delta_{p+q,n} - \delta_{p,n} - \delta_{q,n}) \times \\ &\quad (\delta_{p+q,m} - \delta_{p,m} - \delta_{q,m}) \\ &\quad + \delta_{n,m} (k^{\text{on}} b^2 \delta_{n,1} + k^{\text{off}} \bar{x}_n). \end{aligned} \quad (27)$$

Equation (25) is a linear Fokker–Planck equation, which describes the linear-noise approximation, where Π is a Gaussian. Note that the matrix entries $A_{n,m}$ and $B_{n,m}$ are not functions of Ω . From Eq. (25) we obtain the time evolution of the first and second moments of the fluctuation,

$$\frac{\partial \langle \epsilon \rangle}{\partial t} = \mathbf{A} \cdot \langle \epsilon \rangle \quad (28)$$

$$\frac{\partial \langle \epsilon \epsilon \rangle}{\partial t} = \mathbf{A} \cdot \langle \epsilon \epsilon \rangle + \langle \epsilon \epsilon \rangle \cdot \mathbf{A}^T + \mathbf{B}. \quad (29)$$

Equations (28) and (29) are used in “Low confinement: the linear-noise approximation” in Section “Results” to analytically compute the autocorrelation function.

The solution of Eq. (28) with initial condition $\langle \epsilon \rangle(0) = \mathbf{0}$ is $\langle \epsilon \rangle(t) \equiv \mathbf{0}$. Hence

$$\begin{aligned} \frac{d \langle x_n \rangle}{dt} &= k^{\text{on}} b \delta_{n,1} \\ &- \frac{k}{2} \sum_{p=1}^{\lfloor N/2 \rfloor} \sum_{q=p}^{N-p} \langle x_p \rangle \langle x_q \rangle (2 - \delta_{p,q}) \times \\ &\quad (\delta_{p,n} + \delta_{q,n} - \delta_{p+q,n}) \\ &- k^{\text{off}} \langle x_n \rangle + O(\Omega^{-1}). \end{aligned} \quad (30)$$

I.e., in the linear noise approximation the mean obeys the macroscopic rate equation.

Acknowledgements

We thank Dr. Ramon Grima (University of Edinburgh, Scotland) for useful discussions. RR was financed by a grant from the Swiss SystemsX.ch initiative (grant WingX), evaluated by the Swiss National Science Foundation. This project was also supported with a grant from the Swiss SystemsX.ch initiative, grant LipidX-2008/011 to IFS.

References

1. Qian H, Saffarian S, Elson EL (2002) Concentration fluctuations in a mesoscopic oscillating chemical reaction system. *Proc Natl Acad Sci USA* 99: 10376–10381.
2. Kim J, Heslop-Harrison P, Postlethwaite I, Bates DG (2007) Stochastic noise and synchronisation during *Dictyostelium* aggregation make cAMP oscillations robust. *PLoS Comput Biol* 3: 2190–2198.
3. Miller P, Zhabotinsky AM, Lisman JE, Wang XJ (2005) The stability of a stochastic CaMKII switch: Dependence on the number of enzyme molecules and protein turnover. *PLoS Biol* 3: 705–717.
4. Shibata T (2004) Amplification of noise in a cascade chemical reaction. *Phys Rev E* 69: 056218.
5. Grima R, Schnell S (2008) Modelling reaction kinetics inside cells. *Essays Biochem* 45: 41–56.
6. Gardiner CW, McNeil KJ, Walls DF, Matheson IS (1976) Correlations in stochastic theories of chemical-reactions. *J Stat Phys* 14: 307–331.
7. Nishikawa M, Shibata T (2010) Nonadaptive fluctuation in an adaptive sensory system: Bacterial chemoreceptor. *PLoS ONE* 5: e11224.
8. Mouri K, Nacher JC, Akutsu T (2009) A mathematical model for the detection mechanism of DNA double-strand breaks depending on autophosphorylation of ATM. *PLoS ONE* 4: e5131.
9. Perc M, Gosak M, Marhl M (2007) Periodic calcium waves in coupled cells induced by internal noise. *Chem Phys Lett* 437: 143–147.
10. Kurtz TG (1972) Relationship between stochastic and deterministic models for chemical reactions. *J Chem Phys* 57: 2976–2978.
11. Raj A, Peskin CS, Tranchina D, Vargas DY, Tyagi S (2006) Stochastic mRNA synthesis in mammalian cells. *PLoS Biol* 4: 1707–1719.
12. Grima R (2010) An effective rate equation approach to reaction kinetics in small volumes: Theory and application to biochemical reactions in nonequilibrium steady-state conditions. *J Chem Phys* 133: 035101.
13. Beard DA, Qian H (2007) Relationship between thermodynamic driving force and one-way fluxes in reversible processes. *PLoS ONE* 2: e144.
14. Shimoni Y, Altuvia S, Margalit H, Biham O (2009) Stochastic analysis of the SOS response in *Escherichia coli*. *PLoS ONE* 4: e5363.
15. Grima R (2009) Noise-induced breakdown of the Michaelis-Menten equation in steady-state conditions. *Phys Rev Lett* 102: 218103.

16. Perc M, Green AK, Dixon CJ, Marhl M (2008) Establishing the stochastic nature of intracellular calcium oscillations from experimental data. *Biophys Chem* 132: 33–38.
17. Dobrzyński M, Bruggeman FJ (2009) Elongation dynamics shape bursty transcription and translation. *Proc Natl Acad Sci USA* 106: 2583–2588.
18. Luby-Phelps K (2000) Cytoarchitecture and physical properties of cytoplasm: Volume, viscosity, diffusion, intracellular surface area. *Int Rev Cytol* 192: 189–221.
19. Turner MS, Sens P, Socci ND (2005) Nonequilibrium raftlike membrane domains under continuous recycling. *Phys Rev Lett* 95: 168301.
20. Zhao Y, Keen JH (2008) Gyration clathrin: Highly dynamic clathrin structures involved in rapid receptor recycling. *Traffic* 9: 2253–2264.
21. van Dongen PGJ (1987) Fluctuations in coagulating systems. II. *J Stat Phys* 49: 927–975.
22. van Kampen NG (2007) *Stochastic Processes in Physics and Chemistry*. North Holland, 3rd edition.
23. Gillespie DT (1976) A general method for numerically simulating the stochastic time evolution of coupled chemical reactions. *J Comput Phys* 22: 403–434.
24. Ramaswamy R, González-Segredo N, Sbalzarini IF (2009) A new class of highly efficient exact stochastic simulation algorithms for chemical reaction networks. *J Chem Phys* 130: 244104.
25. Ramaswamy R, Sbalzarini IF (2010) Fast exact stochastic simulation algorithms using partial propensities. In: *Proc. ICNAAM, Numerical Analysis and Applied Mathematics, International Conference*. AIP, pp. 1338–1341.
26. Lakowicz JR (2006) *Principles of Fluorescence Spectroscopy*. Springer US. doi:10.1007/978-0-387-46312-4.
27. Gillespie DT (1992) A rigorous derivation of the chemical master equation. *Physica A* 188: 404–425.
28. Leyvraz F (2003) Scaling theory and exactly solved models in the kinetics of irreversible aggregation. *Physics Reports* 383: 95–212.

Figure Legends

Figure 1: Lifetime from the linear noise Fokker–Planck approximation at low confinement. Lifetime (correlation time) as a function of burst for (a) small and (b) large bursts, normalised to the no-burst, unit-stoichiometry case $b = 1$ for monomers $n = 1$, dimers $n = 2$ and trimers $n = 3$. The region above ca. $b = 300$ defines the high- b region, where lifetimes become insensitive to b . Note that the lifetime of monomer decreases whereas that of the dimer and trimer increases.

Figure 2: (Colour) Decay-rate function from the linear noise Fokker–Planck approximation at low confinement. Decay-rate function $\chi_n(t)$ for several burst values b . (a) Monomers $n = 1$. (b) Dimers $n = 2$. (c) Trimers $n = 3$. For dimers and trimers there is a threshold burst above which the $\chi_n(t)$ becomes non-monotonic in t . Furthermore, it develops a maximum and it appears at later times with increase in burst b .

Figure 3: Lifetime from the full-master-equation trajectories. Lifetimes as a function of system volume Ω for constant burst b , each normalised to its corresponding $\Omega = 1000$ system. (a) No burst, $b = 1$. (b) Higher burst, $b = 500$ for monomers $n = 1$, dimers $n = 2$ and trimers $n = 3$. Note that the system becomes insensitive to Ω at large enough Ω , as the linear-noise approximation predicts (see “Low confinement: the linear-noise approximation” in “Results”). As volume decreases, the system departs from linear-noise behaviour. Note that trimers are insensitive to volume as they are not a reactant in a non-linear reaction.

Figure 4: (Colour) Lifetime from the full-master-equation trajectories. Lifetimes normalised to their value at $(b, \Omega) = (1, 1000)$. (a) Monomers $n = 1$, (b) dimers $n = 2$, (c) trimers $n = 3$. N.B.: The void region for small Ω corresponds to population fluctuations becoming larger than the mean. Shown is an interpolation of data sampled at intervals $(\Delta b, \Delta \Omega) = (10, 10)$.

Figure 5: (Colour) Decay-rate function from the full-master-equation trajectories. Decay-rate function $\chi_n(t)$ for (a) monomers $n = 1$, (b) dimers $n = 2$, and (c) trimers $n = 3$ as volume shrinks at $b = 500$. $t_2^{\chi, \max}$ is defined as the position of the maximum. Shrinking volume alone reduces $t_2^{\chi, \max}$, as opposed to increasing b , see Fig. 1. Similar trend is also shown by the trimers.

Figure 6: (Colour) ACF initial curvature from the full-master-equation trajectories. ACF initial curvature, $Z_n \equiv \frac{d^2}{dt^2} C_{nn}(0) = -\frac{d}{dt} \chi_n(0)$, normalised by its absolute value at $(b, \Omega) = (1, 1000)$. (a) Monomers $n = 1$, (b) dimers $n = 2$, (c) trimers $n = 3$. This quantity serves as a lower dimensional read-out of the decay-rate function $\chi_n(t)$. N.B.: The void region for small Ω corresponds to population fluctuations becoming larger than the mean. Shown is an interpolation of data sampled at intervals $(\Delta b, \Delta \Omega) = (10, 10)$.

Tables

Table 1. ACF characteristics upon increasing burst b and confinement Ω^{-1} .

Characteristic	LN approx. ($\Delta_b, \Delta_{\Omega^{-1}}$)	Full master equation ($\Delta_b, \Delta_{\Omega^{-1}}$)
τ_1	$(-, 0)$	$(\smile, +) \blacklozenge$
τ_2	$(+, 0)$	$(+, +)$
τ_3	$(+, 0)$	$(+, 0) \star$
Z_1	$(+, 0)$	$(+, +)$
Z_2	$(-, 0) \blacktriangle$	$(-, +) \blacktriangle \spadesuit$
Z_3	$(-, 0) \blacktriangle$	$(-, +) \blacktriangle \spadesuit$
$t_1^{\chi, \max}$	$(0, 0)$	$(0, 0)$
$t_2^{\chi, \max}$	$(+, 0)$	$(+, -)$
$t_3^{\chi, \max}$	$(+, 0)$	$(+, -)$

Characteristics upon increasing burst b and confinement Ω^{-1} , encoded as pairs $(\Delta_b, \Delta_{\Omega^{-1}})$, where $\Delta_b, \Delta_{\Omega^{-1}} \in \{+, -, 0, \smile\}$ is the modulation of the relevant characteristic as b or Ω^{-1} increases, respectively, while keeping the other constant. Here τ_n is the lifetime, Z_n is the initial curvature of the ACF and $t_n^{\chi, \max}$ is the time at which the decay rate of the ACF is maximum for monomers $n = 1$, dimers $n = 2$ and trimers $n = 3$ (see Section “Model”) The modulation states are positive (+), negative (-), negligible or zero (0), and decreasing-then-increasing (\smile). \blacklozenge : \smile because there exists a competition of burst-induced versus confinement-induced modulation. \star : $\Delta_{\Omega^{-1}} \tau_n \equiv 0$ for species reacting only unimolecularly. \blacktriangle : $\Delta_b Z_n$ decreases from positive to negative, reflecting the role of burst in changing $\chi_n(t)$ monotonicity. \spadesuit : $\Delta_{\Omega^{-1}} Z_n$ does not change sign, hence Ω^{-1} does not change $\chi_n(t)$ monotonicity.

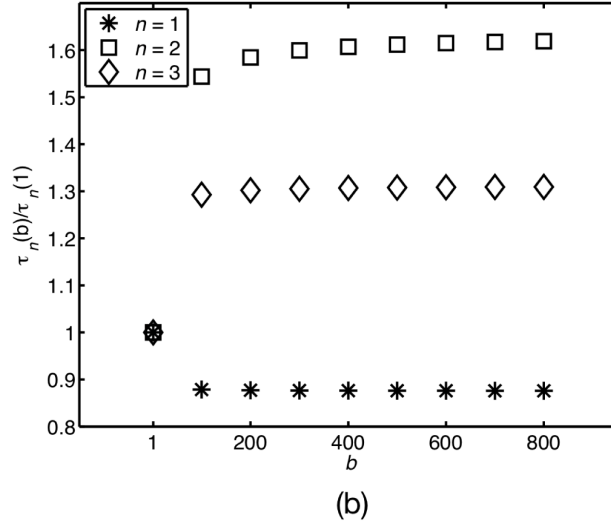
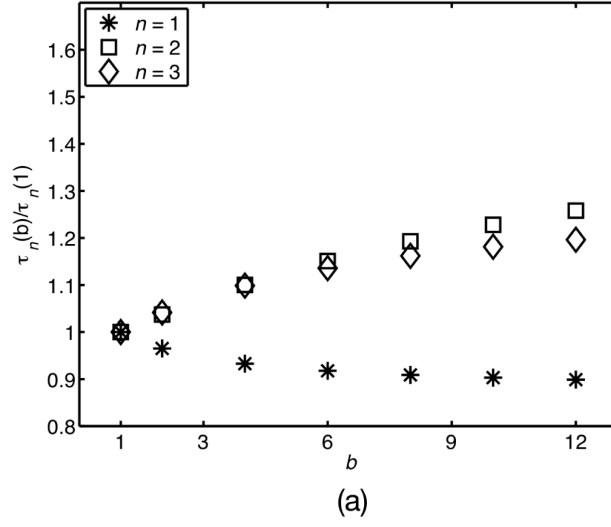


Figure 1. Lifetime from the linear noise Fokker–Planck approximation at low confinement. Lifetime (correlation time) as a function of burst for (a) small and (b) large bursts, normalised to the no-burst, unit-stoichiometry case $b = 1$ for monomers $n = 1$, dimers $n = 2$ and trimers $n = 3$. The region above ca. $b = 300$ defines the high- b region, where lifetimes become insensitive to b . Note that the lifetime of monomer decreases whereas that of the dimer and trimer increases.

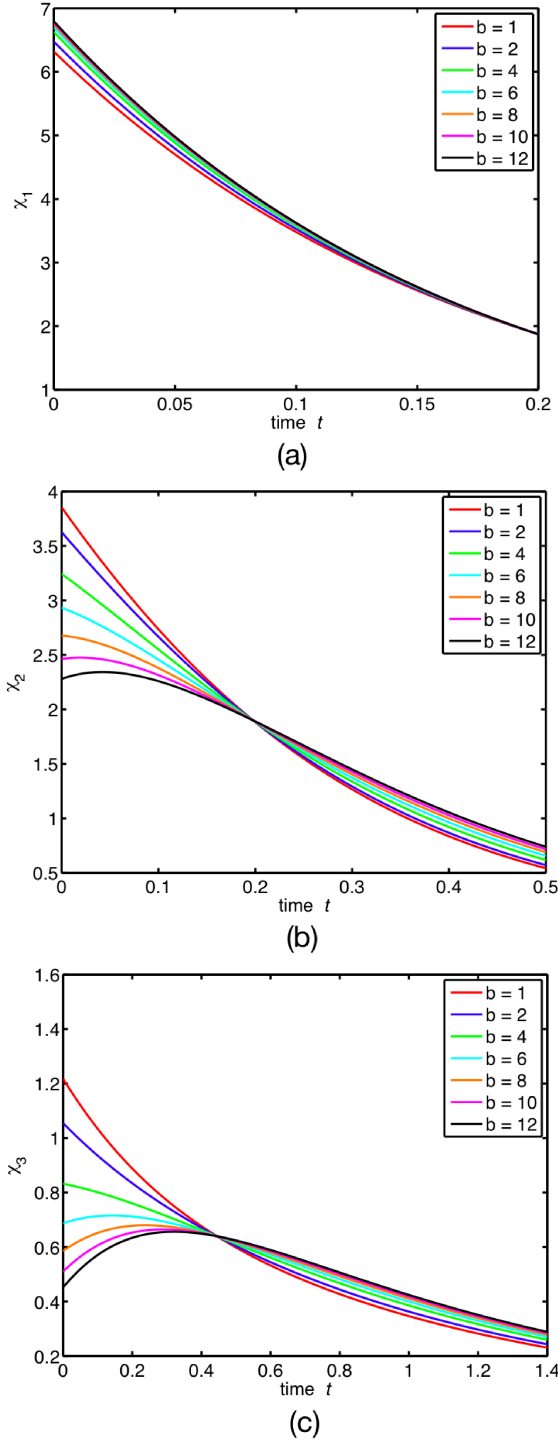


Figure 2. (Colour) **Decay-rate function from the linear noise Fokker–Planck approximation at low confinement.** Decay-rate function $\chi_n(t)$ for several burst values b . (a) Monomers $n = 1$. (b) Dimers $n = 2$. (c) Trimers $n = 3$. For dimers and trimers there is a threshold burst above which the $\chi_n(t)$ becomes non-monotonic in t . Furthermore, it develops a maximum and it appears at later times with increase in burst b .

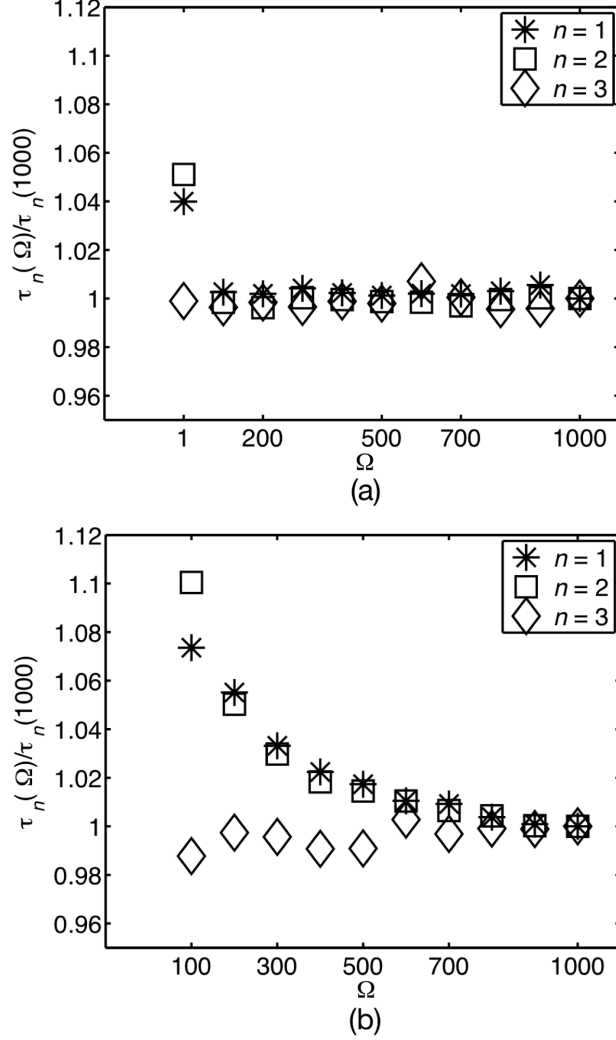


Figure 3. Lifetime from the full-master-equation trajectories. Lifetimes as a function of system volume Ω for constant burst b , each normalised to its corresponding $\Omega = 1000$ system. (a) No burst, $b = 1$. (b) Higher burst, $b = 500$ for monomers $n = 1$, dimers $n = 2$ and trimers $n = 3$. Note that the system becomes insensitive to Ω at large enough Ω , as the linear-noise approximation predicts (see “Low confinement: the linear-noise approximation” in “Results”). As volume decreases, the system departs from linear-noise behaviour. Note that trimers are insensitive to volume as they are not a reactant in a non-linear reaction.

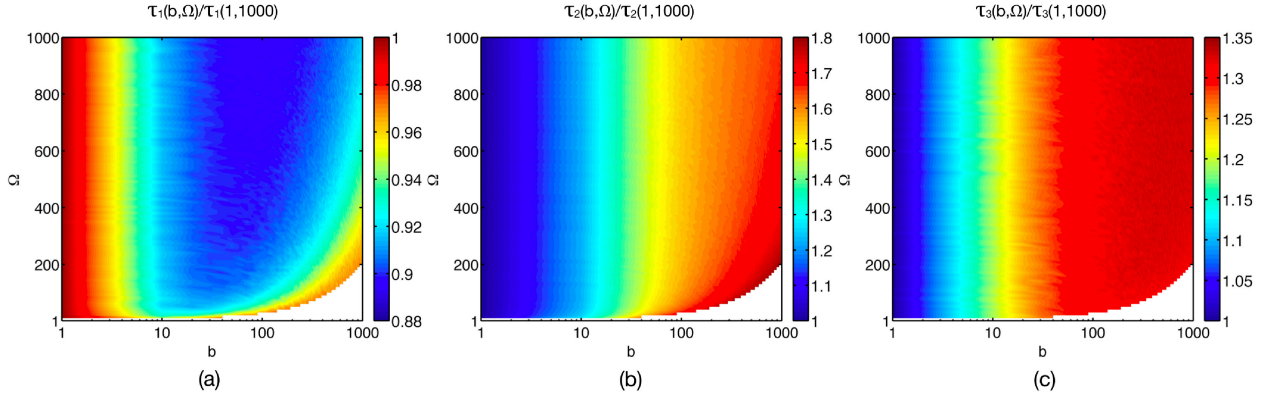


Figure 4. (Colour) **Lifetime from the full-master-equation trajectories.** Lifetimes normalised to their value at $(b, \Omega) = (1, 1000)$. (a) Monomers $n = 1$, (b) dimers $n = 2$, (c) trimers $n = 3$. N.B.: The void region for small Ω corresponds to population fluctuations becoming larger than the mean. Shown is an interpolation of data sampled at intervals $(\Delta b, \Delta \Omega) = (10, 10)$.

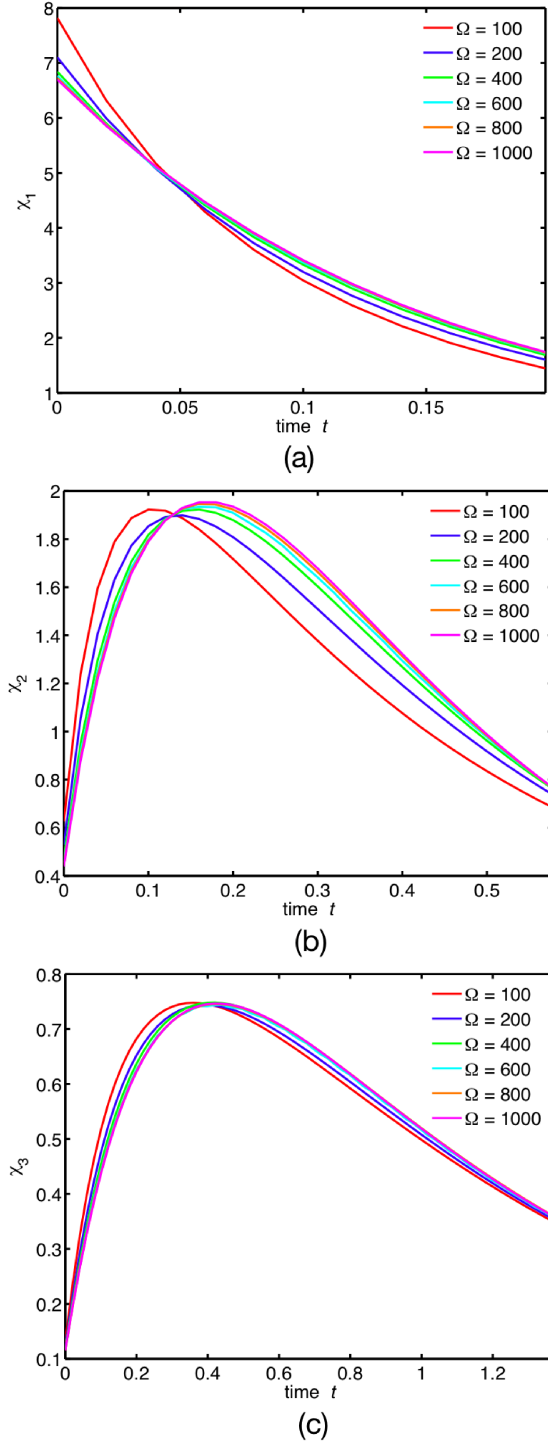


Figure 5. (Colour) **Decay-rate function from the full-master-equation trajectories.** Decay-rate function $\chi_n(t)$ for (a) monomers $n = 1$, (b) dimers $n = 2$, and (c) trimers $n = 3$ as volume shrinks at $b = 500$. $t_2^{\chi, \max}$ is defined as the position of the maximum. Shrinking volume alone reduces $t_2^{\chi, \max}$, as opposed to increasing b , see Fig. 1. Similar trend is also shown by the trimers.

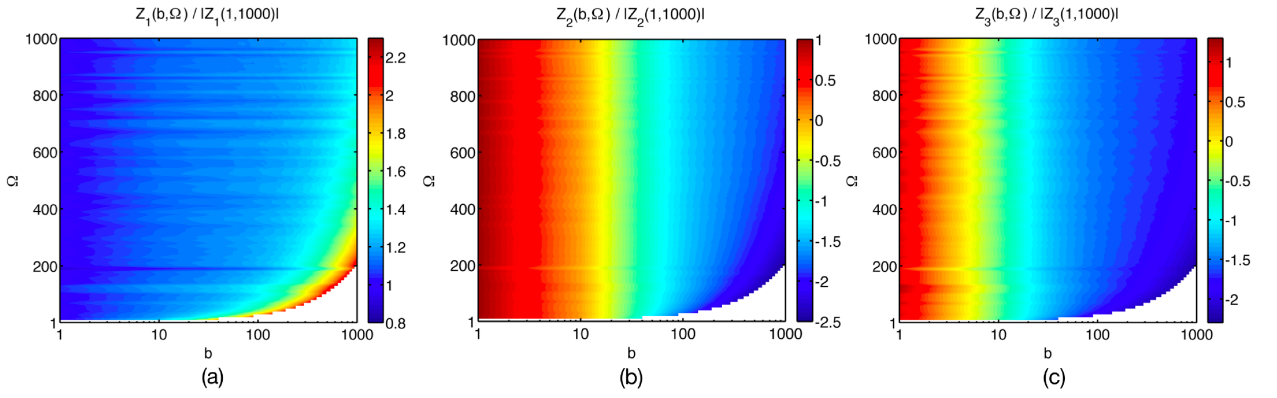


Figure 6. (Colour) **ACF initial curvature from the full-master-equation trajectories.** ACF initial curvature, $Z_n \equiv \frac{d^2}{dt^2} C_{nn}(0) = -\frac{d}{dt} \chi_n(0)$, normalised by its absolute value at $(b, \Omega) = (1, 1000)$. (a) Monomers $n = 1$, (b) dimers $n = 2$, (c) trimers $n = 3$. This quantity serves as a lower dimensional read-out of the decay-rate function $\chi_n(t)$. N.B.: The void region for small Ω corresponds to population fluctuations becoming larger than the mean. Shown is an interpolation of data sampled at intervals $(\Delta b, \Delta \Omega) = (10, 10)$.